Catalytic activity of Cu/η-Al2O3 catalysts prepared from aluminum scraps in the NH3-SCO and in the NH3-SCR of NO

Nawel Jraba, Thabet Makhlouf, Gérard Delahay, Hassib Tounsi

Catalytic activity of Cu/η-Al_2O_3 catalysts prepared from aluminum scraps in the NH_3-SCO and in the NH_3-SCR of NO

Nawel Jraba [a,*], Thabet Makhlouf [a, ‡], Gerard Delahay [b], HassibTounsi [c]

[a)] *Laboratory of Georesources, Materials, Environments and Global Changes, Faculty of Sciences of Sfax, University of Sfax, TUNISIA.*

[b)] *ICGM, Univ Montpellier, ENSCM, CNRS, Montpellier, FRANCE.*

[c)] *Laboratory of Advanced Materials, National School of Engineers of Sfax, University of Sfax, TUNISIA.*

* Corresponding author, *phone number :(+216) 96285898, E-mail address:naweljraba@hotmail.fr*

‡This paper is dedicated to the memory of our dear colleague, Prof. Thabet Makhlouf, who passed away in March 19, 2020.

Abstract

Copper loaded η-alumina catalysts with different copper contents were prepared by impregnation/evaporation method. The catalysts were characterized by XRD, FTIR, BET, UV–vis, H_2-TPR and evaluated, for the first time, in the selective catalytic reduction of NO by NH_3 and in the selective catalytic oxidation of NH_3. The characterization techniques showed that the impregnation/evaporation method permits to obtain highly dispersed copper oxide species on the η-alumina surface when low amount of copper is used (1wt. % and 2 wt.%). The wet impregnation method made it possible to reach a well dispersion of the copper species on the surface of the alumina for the low copper contents Cu(1)-Al_2O_3 and Cu(2)-Al_2O_3. The latter justifies the similar behavior of Cu(1)-Al_2O_3) and Cu(2)-Al_2O_3 in the selective catalytic oxidation of NH_3 where these catalysts exhibit a conversion of NH_3 to N_2 of the order of 100% at T> 500 °C.

Keywords: Cu/η-Al_2O_3; NH_3-SCR; NH_3-SCO; H_2-TPR; TEM

1 Introduction

The selective catalytic reduction (SCR) of NO by ammonia in the presence of excess oxygen is considered a mature technology for the removal of NO from stationary sources (Forzatti, 2001; Usberti et al. 2015). Moreover, this technology has been adapted for the modern diesel exhaust after treatment system using urea as the ammonia precursor (urea-SCR) (Goldbach et al., 2017; Jung et al., 2017; Kröcher, 2018; Nova and Tronkoni, 2014; Piumetti et al., 2015; Yuan et al., 2015). This system contains besides the urea delivery device, a catalyst for the selective catalytic reduction of NO with NH_3 (NH_3-SCR) combined with an ammonia slip catalyst (ASC) for the selective catalytic oxidation of ammonia (NH_3-SCO) (Piumetti et al., 2015; Walker, 2016).

Vanadium-based catalysts (V-catalysts) V_2O_5-WO_3/TiO_2 or V_2O_5–MoO_3/TiO_2 are widely employed in stationary applications since the 1970s (Lai and Wachs, 2018). However, the major drawbacks bounded to the toxicity of vanadium and its weaker activity at low temperature limit the utilization of V-catalysts in automotive applications. Besides, some country regulations such as USA forbid the use of V-catalysts for automotive applications. Therefore, Cu/Fe-exchanged zeolites have been reported as alternative to vanadium-based catalysts because they are active and N_2 selective for the NH_3-SCR (Boron et al., 2019; Villamaina et al., 2019; Xin et al., 2018) and for the NH_3-SCO (Jablonska, 2020). Among all the zeolite-catalysts, Cu/Fe-ZSM-5 and Fe/Cu-BEA are the most extensively investigated in the past 30 years (Hamoud et al., 2019; Villamaina et al., 2019; Xin et al., 2018). Copper-based zeolites are usually more active in the low-temperature (<350°C) range while iron-based zeolites are more active at higher temperatures (>350°C). Small-pore zeolite Cu-SSZ-13 has received great attention due to its higher activity and selectivity at low temperatures and improved hydrothermal stability for diesel vehicles. (Gao and Szanyi, 2018; Lambert, 2019; Shibata et al., 2019)

On the other hand, noble metals (Pt, Pd, and Rh) supported on metal oxides have been studied for the diesel exhaust after treatment system. Common metal oxides such as Al_2O_3, SiO_2, CeO_2, TiO_2, and ZrO_2 are used as support materials for the diesel oxidation catalyst (Jablonska, 2015;

Sun et al., 2019). Nevertheless, γ-Al_2O_3 due to its high surface area (100–200 m^2/g) and its good thermal stability is preferred to all other metal oxides (Kong et al., 2020; Panahi and Delahay, 2017). For instance, Pt-γ-Al_2O_3 is used in the diesel oxidation catalyst (DOC) and ammonia slip catalyst (ASC) (svintsitskiy et al., 2020). The DOC oxidizes CO, unburnt hydrocarbons and NO in the exhaust gas to CO_2, H_2O and NO_2, respectively. The ASC removed the excess of NH_3 by selective catalytic oxidation (SCO) with oxygen to N_2 and H_2O. Pt-γ-Al_2O_3 catalyst is considered to be the most active for ammonia oxidation below 300 °C than the other noble metals (Pd, and Rh). However, Pt-γ-Al_2O_3 catalyst has high selectivity towards N_2O and NO over 300°C (Hansen et al. 2017). The drawbacks of noble-metal catalysts motivate the vehicle manufacturers to reduce their content or substitute them with cheaper Mn/Cu-based oxides catalysts (Damma et al., 2019). Cu based systems are discussed more comprehensively in the review of (Jablonska and Palkovits, 2016). Among Cu based systems, CuO/Al_2O_3 catalyst has been proposed to substitute the noble metal-based emission control catalysts in the NH_3-SCR (Jeong et al., 1999; Kwak et al., 2012; Xie et al., 2004) and NH_3-SCO (Gang et al., 1999; Jablonska et al., 2018; Jablonska, 2015; Strom et al., 2018). In the early research of (Il'chenko and Ivanovna 1976), CuO was found as one of the most efficient oxide in selective ammonia oxidation into nitrogen and water vapour. Further studies over preoxidised polycrystalline copper foil proved that CuO is an active phase for NH_3-SCO (Mayer et al. 2003). However, due to unsatisfying selectivity to N_2, further studies concerning ammonia oxidation were carried out over CuO supported e.g. on Al_2O_3 (Jones et al., 2005). It should be mentioned that all cited studies have used γ-Al_2O_3 to support copper oxide. To our best knowledge, η-Al_2O_3 has never been employed as support for the preparation of CuO/Al_2O_3 catalysts for the NH_3-SCR of NO and for the NH_3-SCO. Gang et al., 1999 studied supported CuO/γ-Al_2O_3 catalysts containing 5, 10 and 15 wt.% of copper . They found that the best catalytic results in the NH_3-SCO were obtained for the sample loaded with 10 wt.% of Cu (90% of NH_3 conversion with 97% selectivity to N_2 at 300°C). This effect was explained by the

formation of the surface $CuAl_2O_4$-like species, active in NH_3-SCO, in the catalyst containing 10 wt.% of copper. Liang et al., 2012 obtained similar results for Cu(10%)/γ-Al_2O_3 catalysts prepared by different copper precursors (nitrate, acetate and sulfate). They showed that a mixture of CuO and $CuAl_2O_4$ species is formed on the various Cu(10%)/γ-Al_2O_3 catalysts.

In our previous work (Jraba et al., 2018), we reported the preparation of γ-Al_2O_3 and η-Al_2O_3 with high surface areas using aluminum chips collected from metal manufacturing industry as starting materials. η-Al_2O_3 and γ-Al_2O_3 were obtained by calcination at 500 °C of bayerite (α-$Al(OH)_3$) and pseudo-boehmite, respectively. γ-Al_2O_3 and η-Al_2O_3 are considered to be the most important among other alumina's due to their high specific surface area (200–500 m^2/g) and acid-base properties. The two alumina polytypes γ-Al_2O_3 and η-Al_2O_3 have the same non-stoichiometric spinel structure. η-Al_2O_3 has a higher population of stronger Lewis acid sites and a slightly higher activity than γ-Al_2O_3 as an acid catalyst (Jraba et al., 2018). On one hand, γ-Al_2O_3 counts for the most important industrial applications as adsorbents, catalysts and catalyst supports but on the other hand the application of η-Al_2O_3 is rarely reported (Peintinger et al., 2014). The literature showed that η-Al_2O_3 is mostly used as catalyst in the dehydration of methanol to Dimethyl Ether (DME) (Osman et al., 2017; Osman et al., 2018; Hoyong et al., 2017). Osman et al., (2017) showed that loading η-Al_2O_3 with 10 wt.% of silver enhanced both surface Lewis acidity and the hydrophobicity of the carrier. Accordingly, they obtained a catalyst with high degree of activity and stability under steady-state conditions for the production of DME. Le et al., (2017) investigated the methanation of CO and CO_2 using Ni catalysts supported by alumina with different crystalline phases (α-Al_2O_3, θ-Al_2O_3, δ-Al_2O_3, η-Al_2O_3, γ-Al_2O_3, and κ-Al_2O_3). Among these catalysts, Ni/θ-Al_2O_3 showed the highest activity for both CO and CO_2 methanation. Nikoofar et al., (2019) published a review which describes the various organic reactions promoted by nano alumina catalysts (η-Al_2O_3, γ-Al_2O_3, θ-Al_2O_3,..) relevant up to 2017.

Herein, CuO/ η-Al_2O_3 catalysts were prepared by impregnation/evaporation method using copper acetate as precursor. Then, these catalysts were tested for the first time in the reactions of

NH_3-SCR of NO and of NH_3-SCO in presence of water vapour. The prepared CuO/ η-Al_2O_3 catalysts were characterized by XRD, SEM, TEM, NH_3-TPD, H_2-TPR, UV-vis and N_2 adsorption-desorption techniques.

2 Experimental

2.1 Preparation of the catalysts

Five copper loaded η-alumina catalysts Cu(x)-Al_2O_3, with x theoretical copper loadings were prepared by wet impregnation/evaporation technique. In a flask containing 100 mL of distilled water, the desired amount of copper acetate $Cu(CO_2CH_3)_2.H_2O$ (Sigma Aldrich, ACS reagent, ≥ 98%) was added to obtain the copper contents of 1 wt.%, 2 wt.%, 3wt.%, 5 wt.% and 7.5 wt%. After the total dissolution of the copper acetate, a mass of 1.5 g of alumina η-Al_2O_3 was added. The flask is then mounted on a rotary evaporator and the suspension is stirred for 4 hours at 80 ° C. After this step, the water was evaporated under reduced pressure for about 1 hour. Once dry, the solid was placed in an oven at 80 °C overnight and finally calcined at 500 °C under an air stream (2 °C/min) for 10 hours. In **figure 1** are reported the photographs of the prepared catalysts.

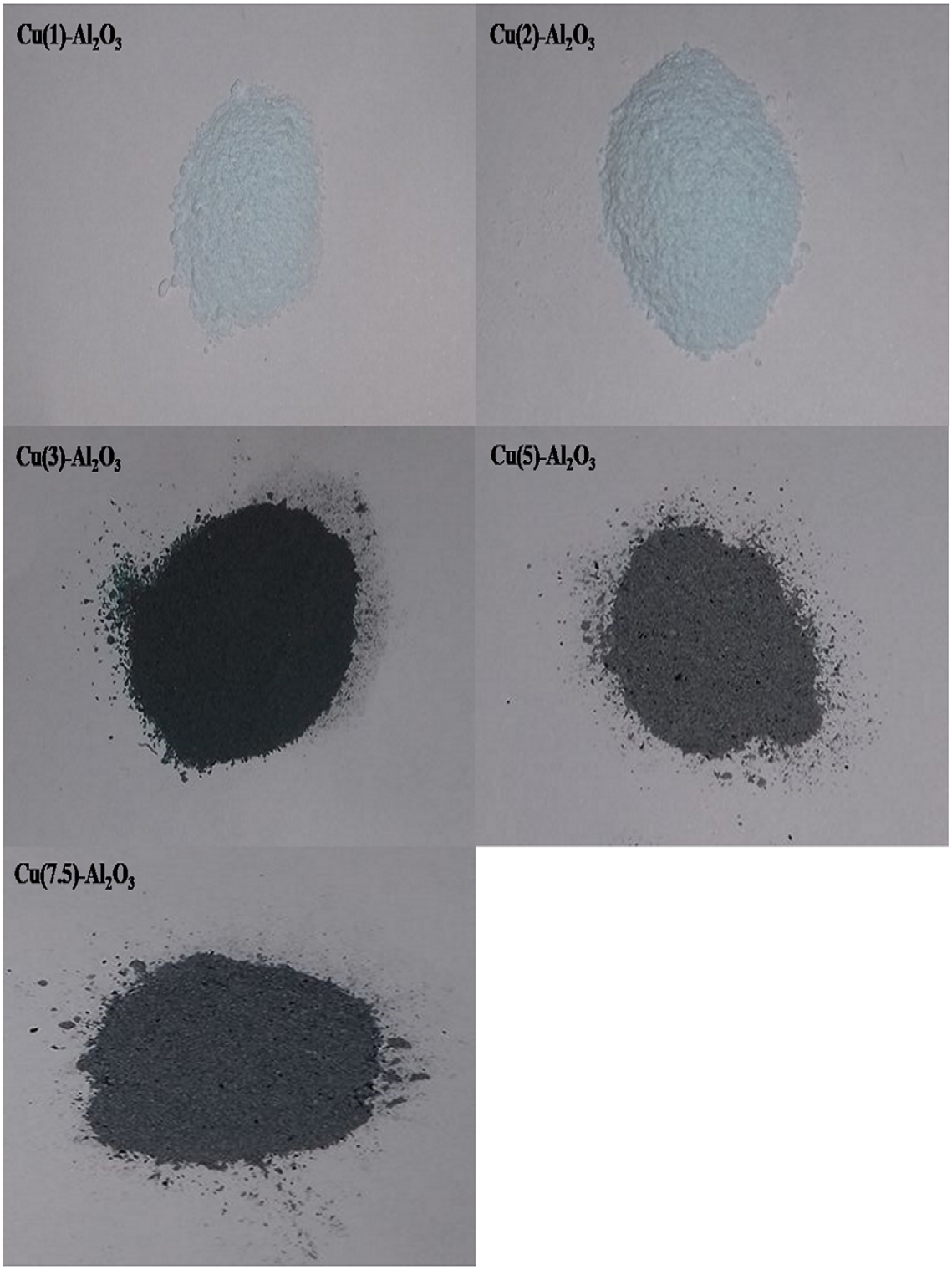

Figure 1: Colors of the prepared catalysts after copper loading and calcination.

2.2 Characterization of Cu(x)-Al_2O_3 catalysts

X-ray powder diffraction patterns were obtained using a D8 ADVANCE BRUKER 40 Kv 40 mA Detector Lynx eye Geometrie Bragg Brenterno (ICGM MAES) using Cu Kα (λ = 0.15418 nm) incident radiation. The diffractograms were recorded at room temperature (RT) between 4° and 70 ° counted in 2θ at a scan speed of 0.02°/s.

The textural properties, surface area and porosity of the support and the catalysts were determined from nitrogen adsorption–desorption isotherms measured at -196 °C using the "micrometrics Tristar Surface Area and Porosity analyzer". The sample (approximately 100 mg) was weighed exactly in a glass tube lined with an "insert" to reduce the void volume. Before all measurements, the samples were treated under high vacuum overnight at 150 °C.

H_2-TPR profiles were carried out with an automated Micromeritics Autochem 2910 analyzer. Before H_2-TPR measurements, samples (50 mg) were pretreated in a quartz U-tube reactor under 5%O_2/He flow (30 cm^3/min) at 550 °C (10 °C/min) for 30 min and then cooled under helium to 60 °C. The samples were then reduced from 60 °C to 800 °C (5 °C/min) under 3% H_2/Ar atmosphere (30 cm^3/min). The reduction gas H_2/Ar, was passed after the reactor through a freezing trap (propan-2-ol + liquid nitrogen) kept at -80°C to remove the formed water. Hydrogen consumption was monitored continuously by a thermal conductivity detector.

The ammonia desorption programmed as a function of the temperature (NH_3-TPD) was carried out using the same H_2-TPR equipment. A mass of 30 mg of catalyst is pretreated at 450 °C for 30 min, under air flow (30 cm^3/min), then saturated with ammonia at 100 °C and purged with helium for 45 min. Following this adsorption, the physisorbed ammonia is removed by leaving the sample for 2 h at 100 °C, under a helium flow rate of 30 cm^3/min. Finally, the temperature was raised to 550 °C (10 °C/min), under a helium flow rate of 30 cm^3/min.

The Selective Catalytic Reduction of NO by NH_3 was carried out in a fixed-bed quartz flow reactor operating at atmospheric pressure. The catalyst (24 mg) was activated in-situ at 550°C for 1 hour under a flow of O_2/He (20/80, v/v) and then cooled to 180°C. A feed mixture of

1000 ppm NO, 1000 ppm NH_3, 8% O_2 in He and 3.5% H_2O was then passed through the catalyst at a flow rate of 100 cm^3/min (GHSV = 250000 cm^3/g. h). The NH_3-SCR was carried out on programmed temperature from 180 °C to 500 °C with the heating rate of 5 °C/min.

For the Selective Catalytic Oxidation of ammonia (NH_3-SCO), the test was carried out on the catalysts already tested in the NH_3-SCR of NO. At 550 °C, the NO flow is cut off and the NH_3-SCO experiments were carried out adjusting He flow and by decreasing the temperature from 500 °C to 180 °C with the heating rate of 5 °C/ min.

The reactants and products were analysed by a quadruple mass spectrometer (Pfeiffer Omnistar) equipped with Channeltron and Faraday detectors (0–200 amu) following these characteristic masses: NO (30), N_2 (14, 28), N_2O (28, 30, 44), NH_3 (15, 17, 18), O_2 (16, 32) and H_2O (17, 18).

The percentages of NO (X_{NO}) and NH_3 (X_{NH3}) conversions were calculated on the basis of the differences in their concentrations measured before and after the catalyst bed.

$$X_{NO} = \frac{(NO)_0 - (NO)_T}{(NO)_0} \times 100$$

$$X_{NH3} = \frac{(NH_3)_0 - (NH_3)_T}{(NH_3)_0} \times 100$$

3 Results and discussion

3.1 Characterization of the catalysts

The XRD patterns of the support η-Al_2O_3, CuO (Sigma Aldrich, ACS reagent 99.0 %) and the prepared catalysts Cu(x)-Al_2O_3 are shown in **figure 2**. The characteristic peaks at angles in 2θ 19.5°, 37.5°, 39.7°, 45.8°, 60.8° and 67.2° correspond to η-Al_2O_3 phase having spinel lattice (JCPDS, No. 04-0875). The introduction of copper leads to the destruction of the structure of η-Al_2O_3 for the catalysts with higher copper contents Cu(3)-Al_2O_3, Cu(5)-Al_2O_3 and Cu (7.5)-Al_2O_3.

These catalysts showed the characteristic peaks of CuO (JCPDS, No. 80-0076) at the angles in 2θ 32.6°, 35.6°, 38.8° and 48.8°, 58.3° and 61.5° (Liang et al., 2012). On the other hand, for the Cu(1)-Al_2O_3 and Cu(2)-Al_2O_3 catalysts, there is a slight decrease in the intensity of the peaks of the support and particularly the peak at 19.5 ° and the absence of the diffraction peaks of CuO. It appears that the copper species present in the Cu(1)-Al_2O_3 and Cu (2)-Al_2O_3 catalysts are small and well dispersed on the surface of the support. Friedman et al., (1978) showed that the saturation of the CuO/ γ-Al_2O_3 catalyst surface a CuO monolayer occurs for a Cu content of about 4-5% by weight for every 100 m^2/g of alumina. Beyond this threshold, crystalline CuO was observed.

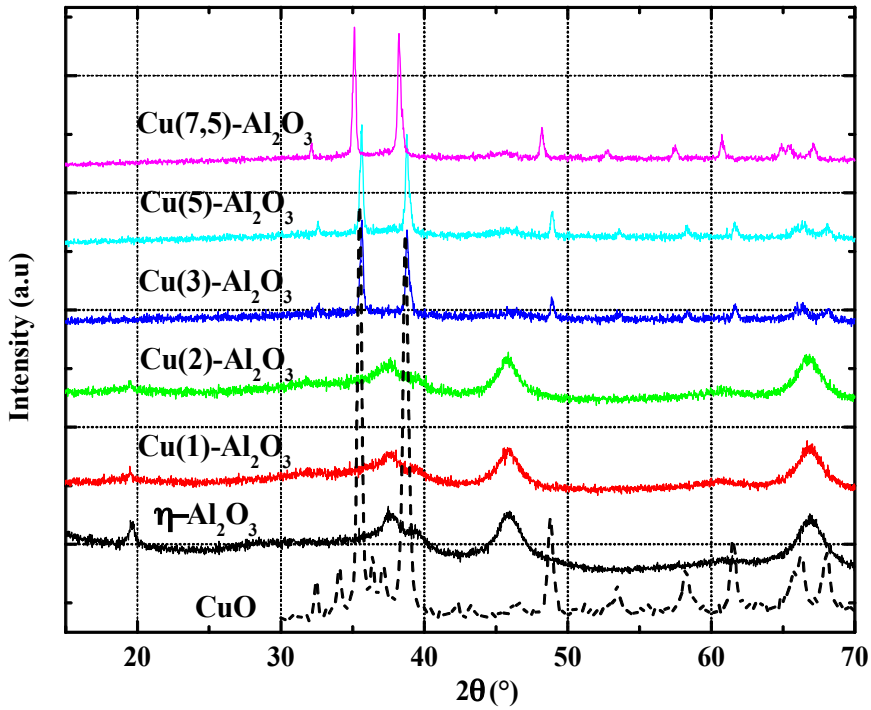

Figure 2: XRD patterns of η-Al_2O_3, CuO and the prepared catalysts Cu(x)-Al_2O_3.

The SEM micrographs of the η-Al_2O_3 and the catalysts Cu(2)-Al_2O_3 and Cu(3)-Al_2O_3 are illustrated in **figure 3**. The SEM micrograph of alumina η-Al_2O_3 is made up small agglomerate particles. The introduction of copper leads to a change in the morphology of η-Al_2O_3 particles. For example, the Cu(2)-Al_2O_3 catalyst presents a sponge-like morphology, which reveals a high level of porosity. On the other hand, for the Cu(3)-Al_2O_3 catalyst, one can see two phases. The

first one is relative to sintered alumina particles and the second is related to CuO particles. It appears that high levels of copper favor the sintering of alumina at lower temperatures than usual. Sintering leads to the drop of the specific surface and the deterioration of the dispersion state of the copper species on the surface of the support.

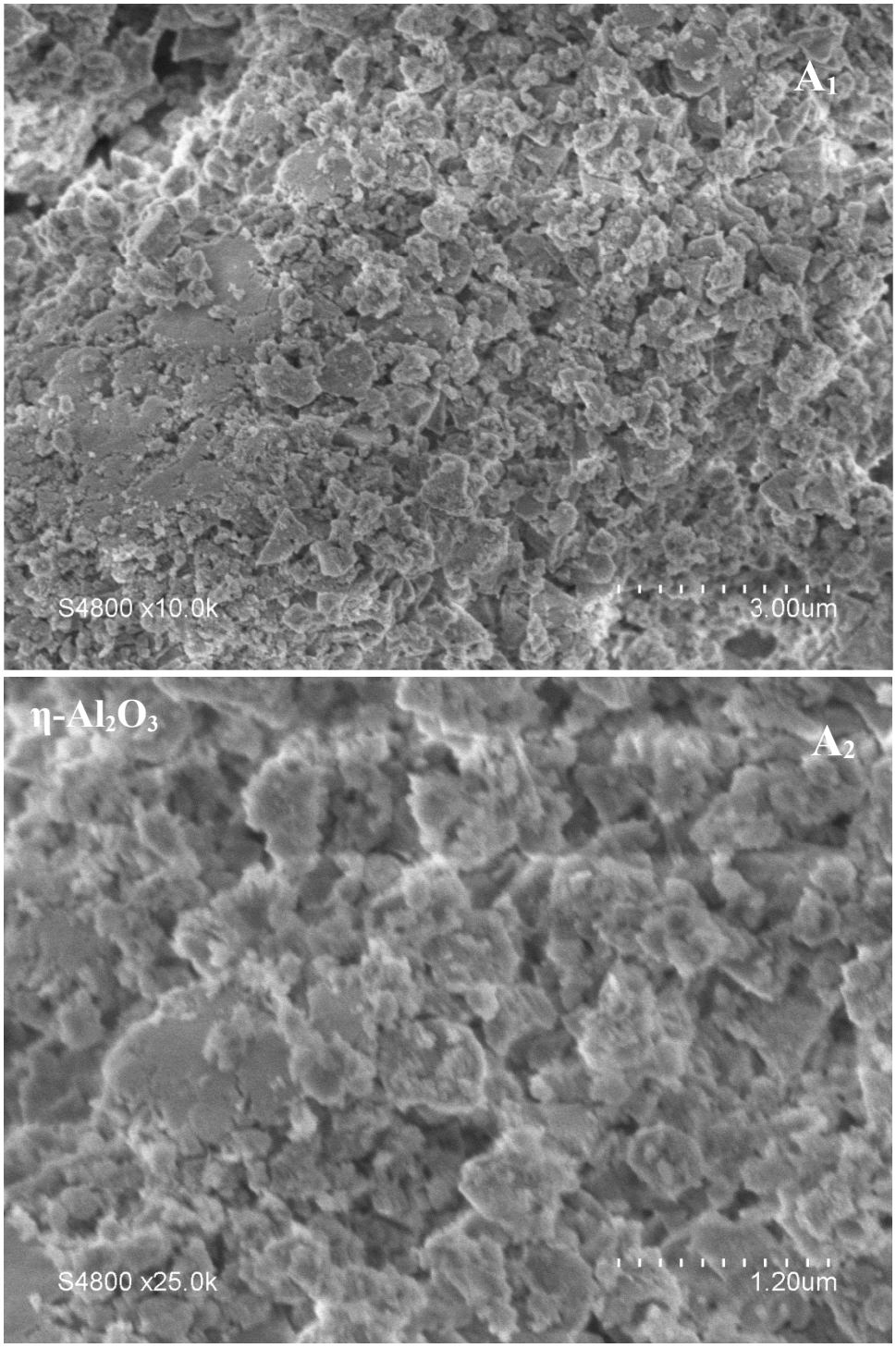

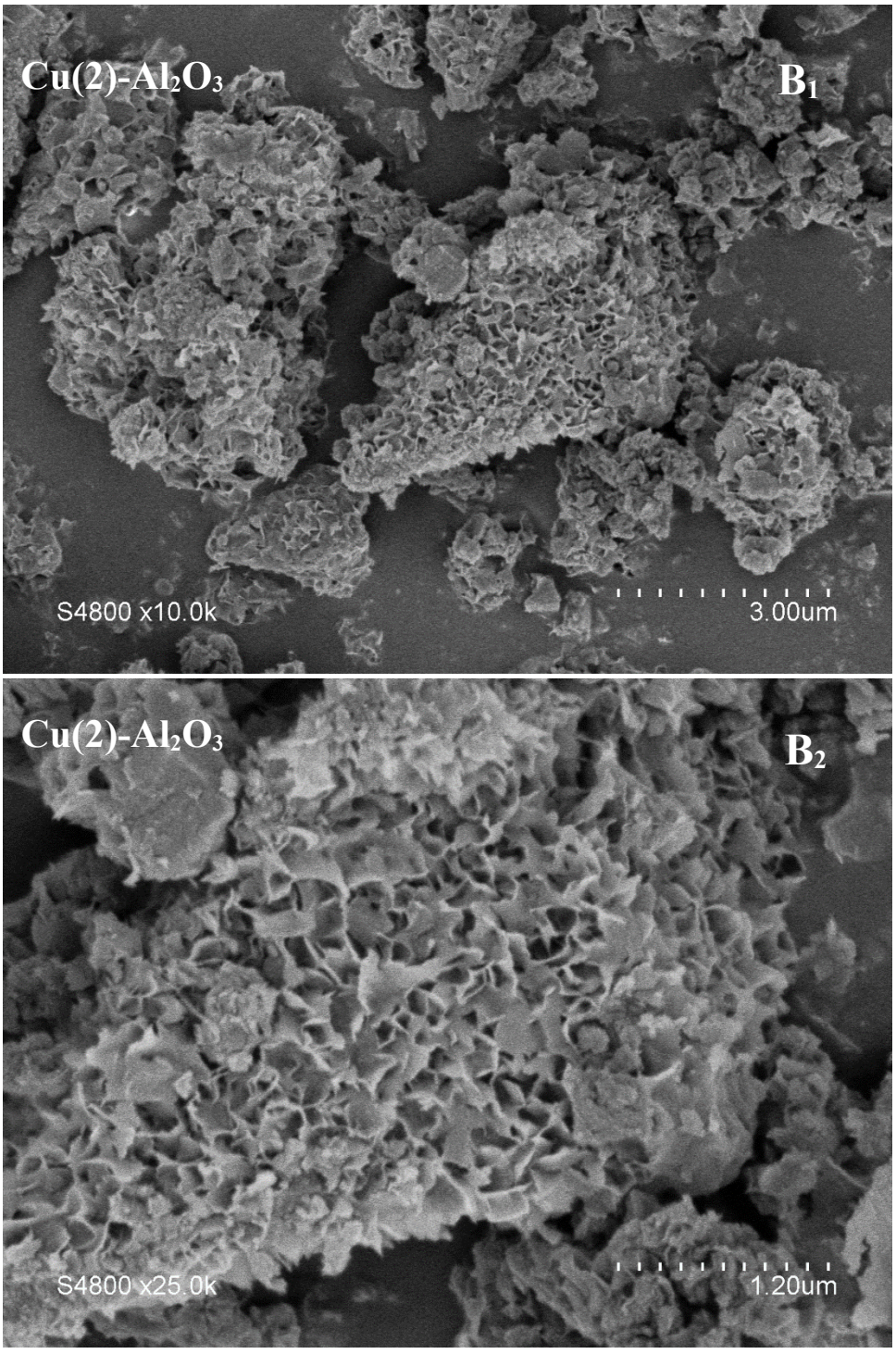
Cu(2)-Al2O3
B1
S4800 x10.0k
3.00um
Cu(2)-Al2O3
B2
S4800 x25.0k
1.20um

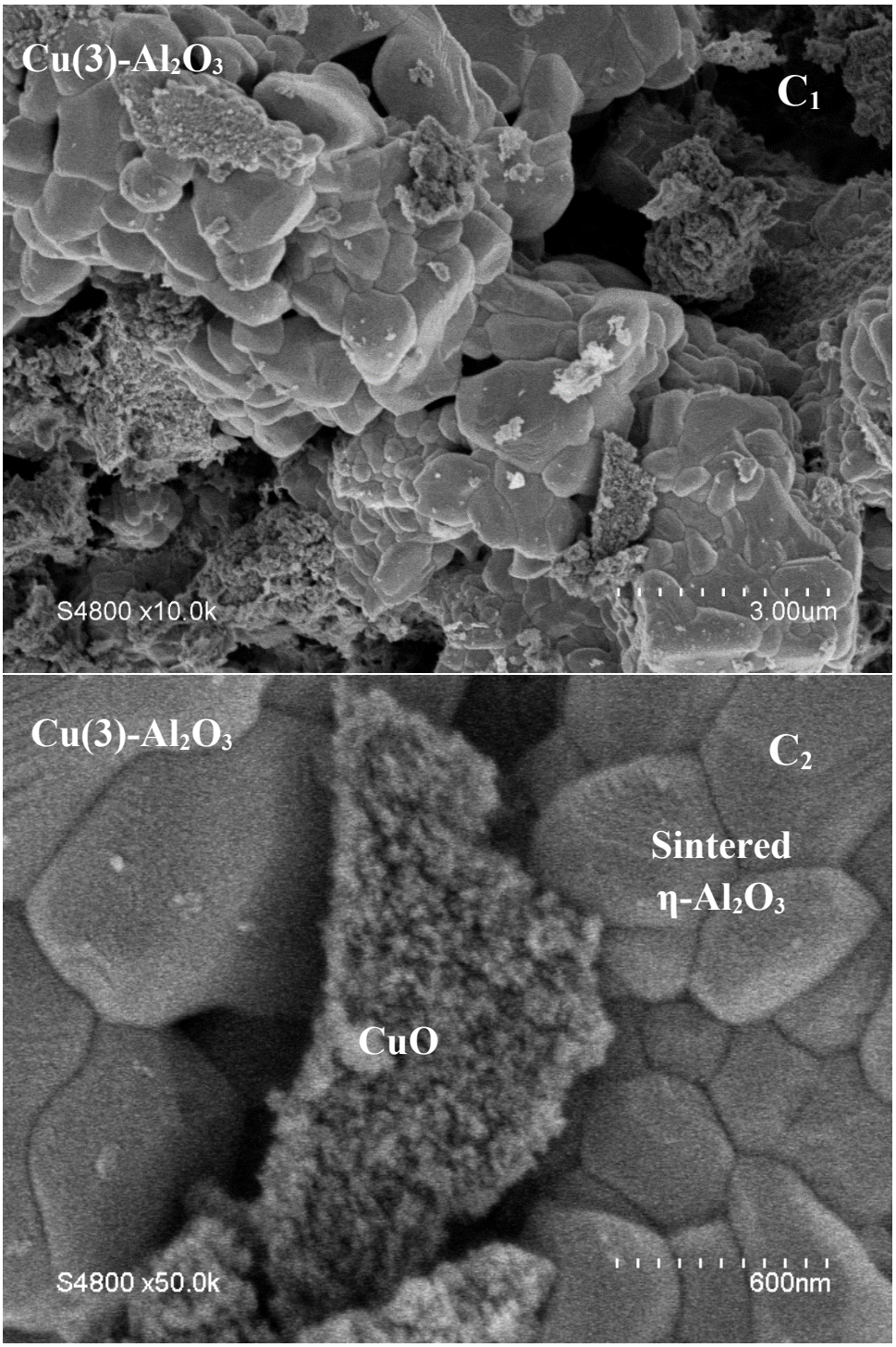

Figure 3: SEM images of the support η-Al_2O_3 (**A_1, A_2**) and the catalysts Cu(2)-Al_2O_3 **(B_1, B_2),** Cu(3)-Al_2O_3 **(C_1, C_2)** with different magnifications.

The TEM images of the Cu(1)-Al_2O_3, Cu(2)-Al_2O_3 and Cu(3)-Al_2O_3 catalysts are reported in **figures 4**. For (Cu(1)-Al_2O_3 catalyst, we note that the copper particles are very small and well dispersed on the support η-Al_2O_3. The increase of the amount of copper leads to the increase of copper species size. For Cu(2)-Al_2O_3 catalyst, copper particles have size about 5-10 nm. Whereas for the Cu(3)-Al_2O_3 catalyst, we note the presence of black spherical particles exceeding 70 nm attributed to copper oxide CuO as shown by XRD.

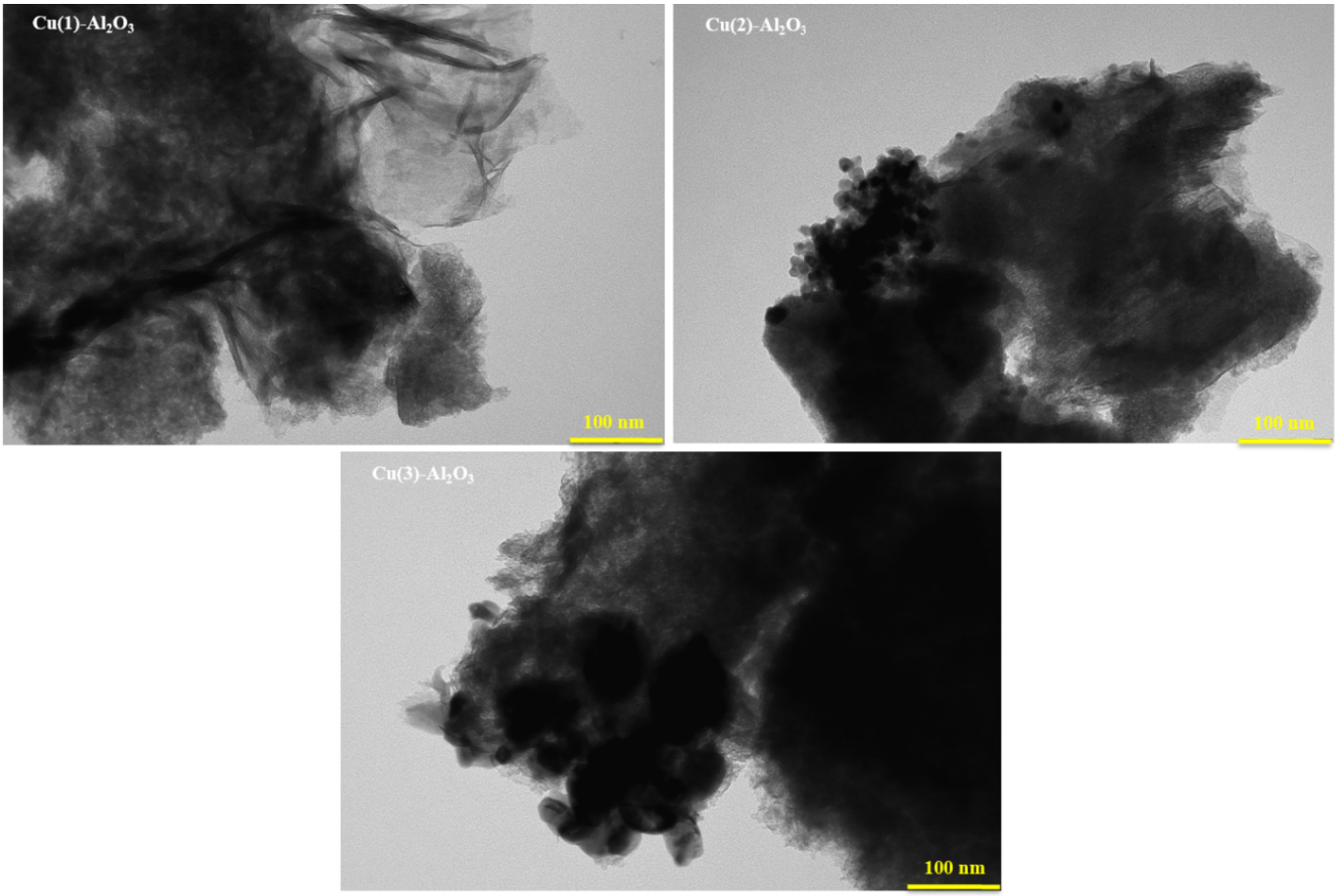

Figure 4: TEM images of Cu(1)-Al_2O_3 Cu(2)-Al_2O_3 and Cu(3)-Al_2O_3 catalysts.

Textural properties of the support η-Al_2O_3 and the prepared catalysts Cu(x)-Al_2O_3 are presented in **Table 1** and **figure 5**. It is noted that the specific surface area S_{BET} of the catalysts decrease after the wet impregnation/evaporation with copper acetate. For example, the specific surface area of the support (S_{BET} = 417 m^2/g) decreases by 18% when 1% of copper was added

(S_{BET} = 343 m^2/g) and 60% with the higher content of copper 7.5% (S_{BET} = 169 m^2/ g). Indeed, the XRD technique has shown that Cu(3)-Al_2O_3, Cu(5)-Al_2O_3 and Cu(7.5)-Al_2O_3 catalysts contain large CuO particles which block the porous structure of η-Al_2O_3. On the other hand, for Cu(1)-Al_2O_3 and Cu (2)-Al_2O_3 catalysts the copper species are well dispersed on the surface of the support and the decrease of S_{BET} was moderate (only 16% for Cu(2)-Al_2O_3 catalyst). On the other hand, we notice an increase in the pore volume up to a copper quantity of 2% wt. and then a decrease beyond this value. Actually, the pore volume of the support which was Vp = 0.295 cm^3/g increases by about 30% (V_p = 0.387 cm^3/g) for 1% Cu and 40% (V_p = 0.411cm^3/ g) for 2% Cu. This result could explain the morphology of η-Al_2O_3 and the formation of macropores as shown by SEM technique. On the other hand, increasing the copper content from 3% to 7.5% induces a reduction in the pore volumes of the catalysts due to the sintering of η-Al_2O_3 particles.

In **figure 5** are reported the N_2 adsorption-desorption isotherms of η-Al_2O_3 and Cu(x)-Al_2O_3 catalysts. All adsorption isotherms are of type IV having hysteresis loops characteristics for mesoporous solids (Petitto et al., 2013). Nevertheless, we note that the addition of copper to the η-Al_2O_3 changes the hysteresis loop from H3 to H2(b) type. This behavior could reflect a change in the pore shape and distribution with the introduction of copper. Indeed, H3 type hysteresis loop indicates the presence of narrow slit-like pores particles with internal voids of irregular shape and broad size distribution but the H2(b) hysteresis loop type shows a narrow distribution of pore shape with a wide neck size distribution (Cychosz and Thommes, 2018). Likewise, when the amount of copper increases there is a decrease in the adsorbed volume at low relative pressure (P/P°), indicating the decrease in microporosity and the increase in mesoporosity.

Table 1: Textural parameters of the prepared catalysts Cu(x)-Al_2O_3

Sample	S_{BET} (m^2/g)	BJH Pore volume (cm^3/g)	BJH pore diameter (nm)
η-Al_2O_3	417	0.295	4.50
Cu(1)-Al_2O_3	343	0.387	4.79
Cu(2)-Al_2O_3	351	0.411	4.85
Cu(3)-Al_2O_3	226	0.319	4.27
Cu(5)-Al_2O_3	229	0.229	4.67
Cu(7.5)-Al_2O_3	169	0.165	4.69

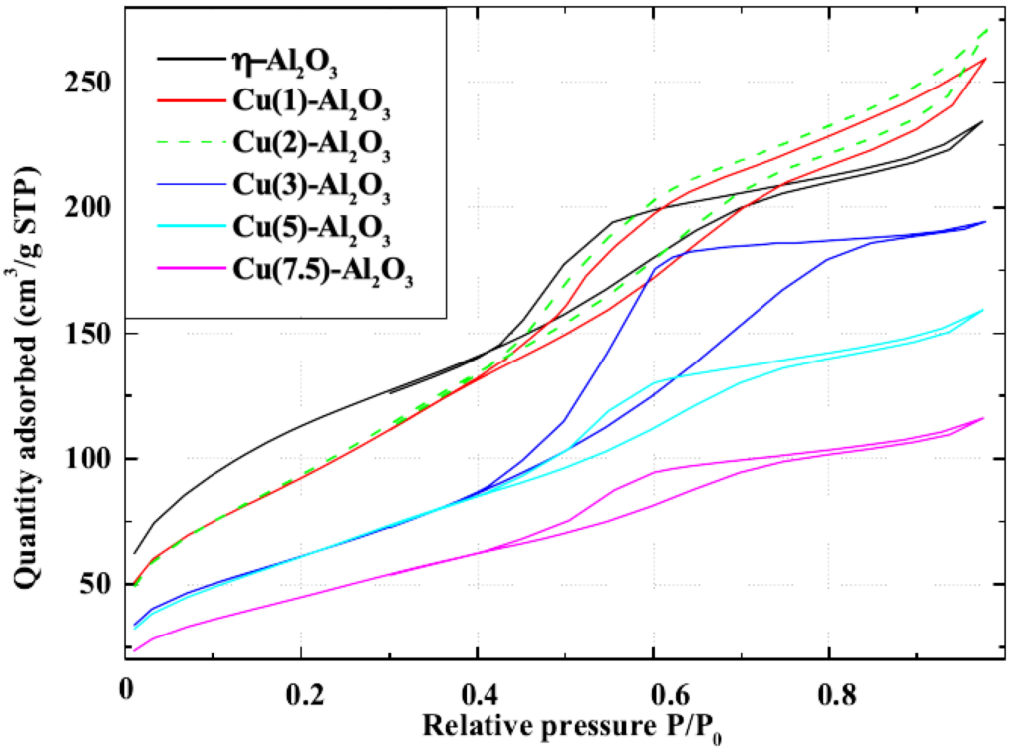

Figure 5: Adsorption–desorption isotherms of η-Al_2O_3 and Cu(x)-Al_2O_3 catalysts.

H_2-TPR profiles of the studied samples are shown in **figure 6**. It is observed that Cu(1)-Al_2O_3 and Cu(2)-Al_2O_3 catalysts have similar reduction profiles. With the increase of copper amount there is an increase of the intensity of the peaks. For Cu(2)-Al_2O_3 catalyst, the first peak around 130 °C was attributed according to Yan et al., (1996) to the reduction of well dispersed CuO clusters on the surface of the support. The second peak extending from 300 °C to 500 °C corresponds to the reduction of highly dispersed Cu^{2+} cations in the structure of the alumina forming a surface spinel $CuAl_2O_4$ type (Aguila et al., 2008; Il'chenko et al., 1976). On the other hand, when the copper content was increased above 3 wt%, there are changes in the catalyst reduction profiles. Indeed, Cu(3)-Al_2O_3, Cu(5)- Al_2O_3 and Cu(7.5)- Al_2O_3 profiles consist only of a broad peak extending from 140–380°C.This reduction peak can be attributed to the reduction of CuO. In fact, Fierro et al., 1994 reported that the supported CuO particle reduction temperature range extends from 200 to 300°C depending on the type of support. The analysis of the deconvolution (not shown) of the reduction profiles of Cu(3)-Al_2O_3, Cu(5)-Al_2O_3 and Cu(7.5)-Al_2O_3 was reported in Table 2. For Cu(3)- Al_2O_3, for example, the central peak was deconvoluted into three peaks. The first is located around 209°C with a relative surface area of around 11%, the second around 232°C (15%) and the last around 274°C. The presence of these peaks could be due to CuO aggregates with different sizes interacting differently with the support.

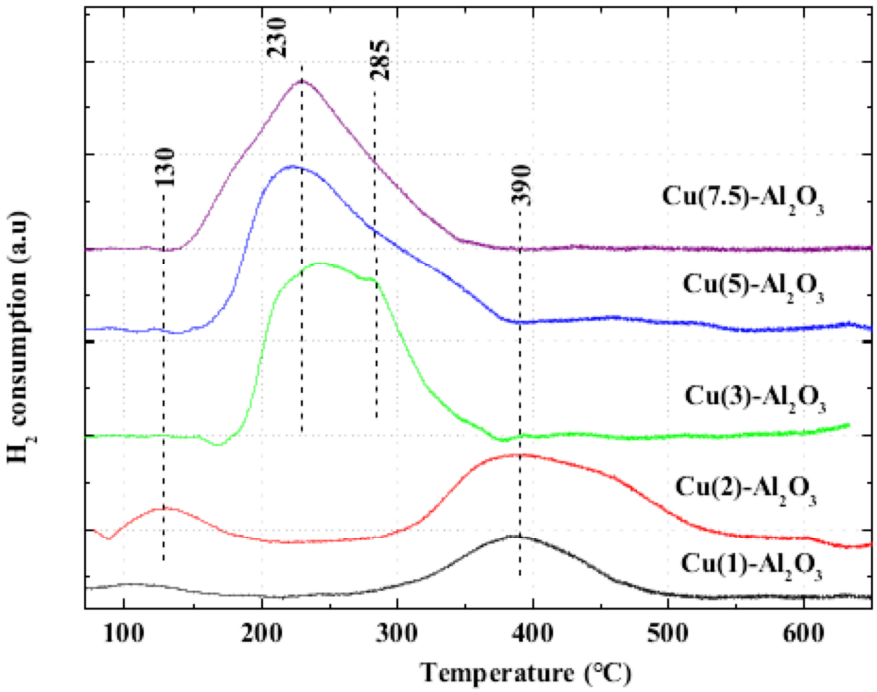

Figure 6: H_2-TPR profiles of Cu(x)-Al_2O_3 catalysts.

Table 2: Results of H_2-TPR profiles deconvolution of Cu(3)-Al_2O_3, Cu(5)-Al_2O_3 et Cu(7.5)-Al_2O_3 catalysts

Catalysts	**Maximum reduction temperature T_m (°C)**		
	Peak I	Peak II	Peak III
Cu(3)-Al_2O_3	209 (11%)	232 (15%)	274 (74%)
Cu(5)-Al_2O_3	_	220 (46%)	282 (54%)
Cu(7.5)-Al_2O_3	179 (11%)	222 (41%)	268 (48%)

The nature and environment of copper species present in the prepared catalysts have been studied by UV-vis spectroscopy. The UV-vis spectra of the carrier η-Al_2O_3 and the Cu(x)-Al_2O_3 catalysts are shown in **figure 7**. Generally, alumina is transparent in the UV-visible range.

Nevertheless, the absorption band around 370 nm of support that could be attributed to impurities. The spectra of the Cu(1)-Al_2O_3 and Cu(2)-Al_2O_3 catalysts have the same profile characterized by a broad absorption band that extends from 350 to 650 nm and centered around 490 nm. This band could be attributed according to the literature (Buvaneswari, 2015; Chaudhary et al., 2018) to CuO or surface spinel type $CuAl_2O_4$ species. The catalysts Cu(3)-Al_2O_3, Cu(5)-Al_2O_3 and Cu(7.5)-Al_2O_3 exhibit characteristic spectra of well-crystallized CuO.

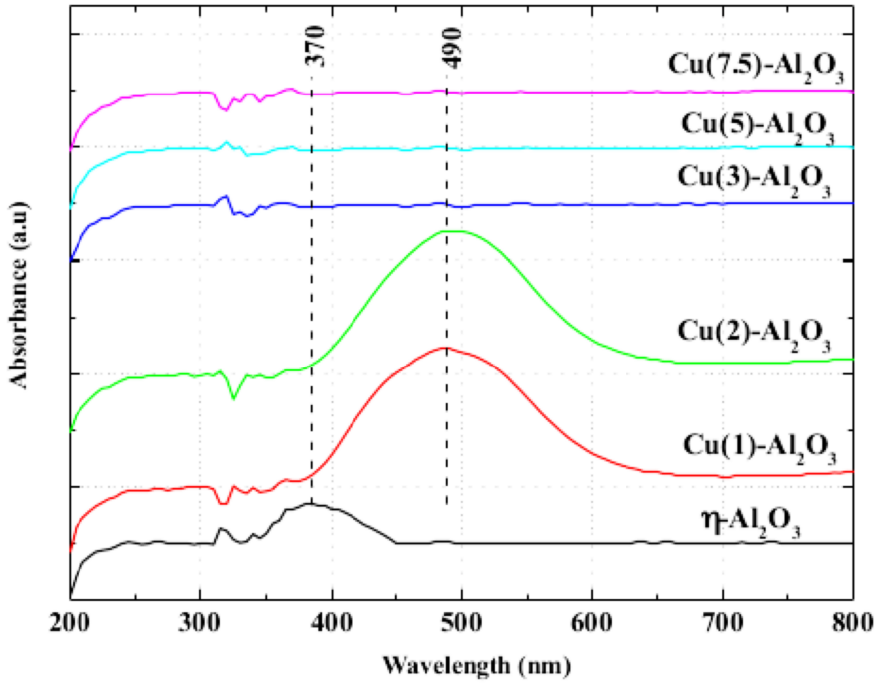

Figure 7: UV-vis spectra of η-Al_2O_3 and Cu(x)-Al_2O_3 catalysts.

The NH_3-TPD profiles of η-Al_2O_3 and the prepared Cu(x)-Al_2O_3 catalysts are reported in **figure 8**. The support η-Al_2O_3 has broad ammonia desorption peak which extends from 110 °C to 475 °C with a maximum at around 180 °C. The catalysts Cu(1)-Al_2O_3 and Cu (2)-Al_2O_3 show similar desorption profiles to the support but with a higher intensity of the peaks. For the other catalysts Cu(3)-Al_2O_3, Cu(5)-Al_2O_3 and Cu(7.5)-Al_2O_3, a peak around 300 °C is observed which increases in intensity with the increase of the copper amounts. Generally, the temperature of desorbed ammonia is related to the strength of acidic sites in the samples. So, according to the maximum desorption temperature of ammonia (T_d) (Carre et al., 2010), there are three types of

acidic sites: *i)* weak acidic sites ($150 \leq T_d$ (°C) ≤ 250), *ii)* average acidic sites ($250 < T_d$ (°C) ≤ 350) *iii)* strong acidic sites T_d (°C) >350. The NH_3 desorption at T ≤150 °C could be attributed to the NH_3 molecules weakly bound to the surface of the support which have not been evacuated at 100 °C.

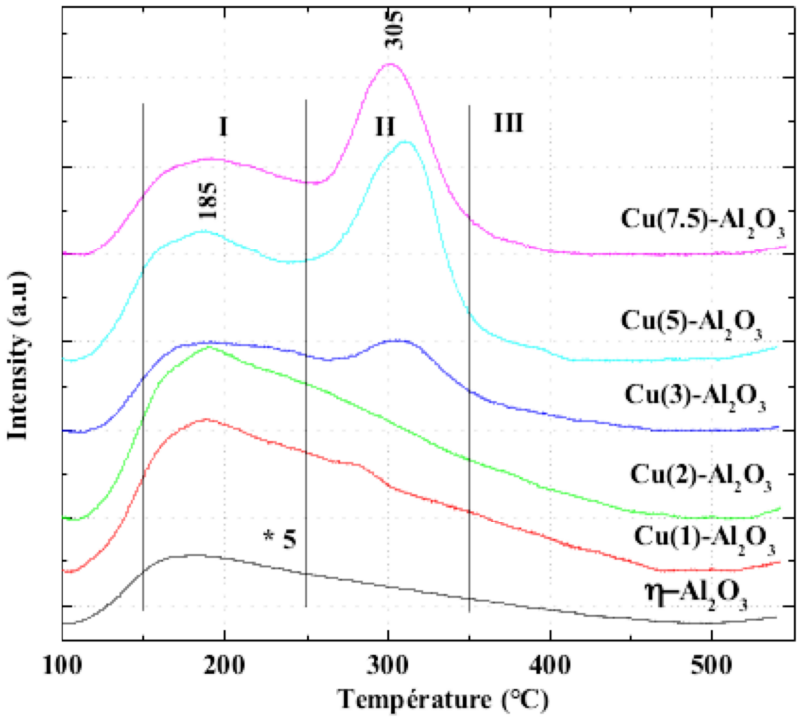

Figure 8: NH_3-TPD profiles of η-Al_2O_3 and Cu(x)-Al_2O_3 catalysts.

3.2 Evaluation of the catalytic activity of Cu(x)-Al_2O_3 catalysts

3.2.1 Selective Catalytic Reduction of NO by NH_3

The prepared catalysts were tested in the NH_3-SCR of NO in the presence of an excess of oxygen and of water vapor according to reaction (I):

$$4NO + 4NH_3 + O_2 \rightarrow 4\,N_2 + 6H_2O \quad \textbf{(I)}$$

In **figures 9** and **10** are reported the NO conversion and NH_3 conversion of the prepared Cu(x)-Al_2O_3 catalysts in the NH_3-SCR of NO. The NO conversion increased initially with increasing temperature, then reached a maximum and decreased. The evolution of the NO conversion passing through a maximum reflects the existence of a competition between two

reactions; the first concerning the reduction of NO and the second the oxidation of NH_3 by the oxygen present in the gas mixture. The competition between the two reactions is in favor of the oxidation of NH_3 at high temperatures which explains the decline in NO conversion. The decrease in the NO conversion is also accompanied with some formation of N_2O according to the two the following reaction:

$$\mathbf{2NH_3 + 2O_2 \rightarrow \ 2N_2O + 3H_2O} \qquad \mathbf{(II)}$$

It should be mentioned that Reaction III implied ammonium nitrate intermediate formed at temperature below 180°C and which starts to decompose above this temperature.

$$\mathbf{4NH_3 + 4NO + 3O_2 \rightarrow \ 4N_2O + 6H_2O} \qquad \mathbf{(III)}$$

Cu(1)-Al_2O_3 and Cu(2)-Al_2O_3 catalysts have similar NO and NH_3 conversion profiles up to 475 °C. Beyond this temperature, the NO conversion decreases for the Cu(2)-Al_2O_3 catalyst, whereas it continues to increase for Cu(1)-Al_2O_3 up to 500 °C where a maximum NO conversion is about 91%. If we look to the conversion of NO to N_2, we notice that these two catalysts are almost selective towards N_2 (**figure 11**), due to the fact that the oxidation of NH_3 is less favored due to the better dispersion of copper. The others catalysts, (Cu(3)-Al_2O_3, Cu(5)-Al_2O_3 and Cu(7.5)-Al_2O_3, display a volcano-shape curve of NO conversion as temperature increases while NH_3 conversion continue to increase with the temperature. For example (**Fig. 9**), the catalyst Cu(7.5)-Al_2O_3 has a maximum NO conversion of the order of 40% at 350 °C which is accompanied with small N_2O production. Therefore, the large drop in NO conversion on this catalyst above 350°C is due to the NH_3 oxidation into NO. Moreover, above 425°C, no NO reduction by ammonia occurs since NO concentration in the outlet gas is superior at the NO concentration in the inlet gas. The behavior of these catalysts could be related to the presence of large CuO particles. One can conclude that the two catalysts Cu(1)-Al_2O_3 and Cu (2)-Al_2O_3 are the most efficient in the reduction of NO by NH_3 in the presence of 3.5% of water vapor. Nevertheless, the Cu(1)-Al_2O_3 has a slightly better NO reduction behavior at high temperature. It has been found that the high

NO conversion of these two catalysts can be related to the presence of small CuO clusters deposited on the surface of η-Al_2O_3 alumina and to $CuAl_2O_4$ surface spinel. We believe that small CuO clusters deposited on the surface and easily reduced at low temperatures are responsible for high temperature N_2 selectivity. In fact, according to the H_2-TPR results, the quantity of these copper species is greater in the case of Cu(2)-Al_2O_3 the and Cu(1)-Al_2O_3 catalysts.

Kwak et al., 2012 investigated the NH_3-SCR of NO reaction under lean conditions on CuO-γ-Al_2O_3 catalysts (350 ppm NO, 350 ppm NH_3, 14% O_2, 2% H_2O, and the balance N_2). They showed that on 10 wt % CuO/γ-Al_2O_3, the NOx conversion is about 30% at 350°C and NH_3 reacts primarily with oxygen to produce NOx. However, on a 0.5 wt CuO/γAl_2O_3 catalyst, NH_3 reacts with NO to form N_2 and the NOx conversion to N_2 was almost 80% at 450 °C. Jeong et al., 1999; carried out the NH_3-SCR of NO over sulphated CuO/γ-Al_2O_3 in a fixed-bed reactor (400 ppm NO, 400 ppm, 4% O_2 and the balanced N_2). They found that the optimum temperatures of the fresh and sulphated CuO/γ-Al_2O_3 in the NH_3-SCR of NO are 350 and 450 °C, respectively. Also, NO conversion over the sulphated catalyst is somewhat higher than that over the fresh catalyst. The amount of N_2O formation in NO reduction over the fresh and the bulk sulphated catalysts is below 10% of NO in the feed.

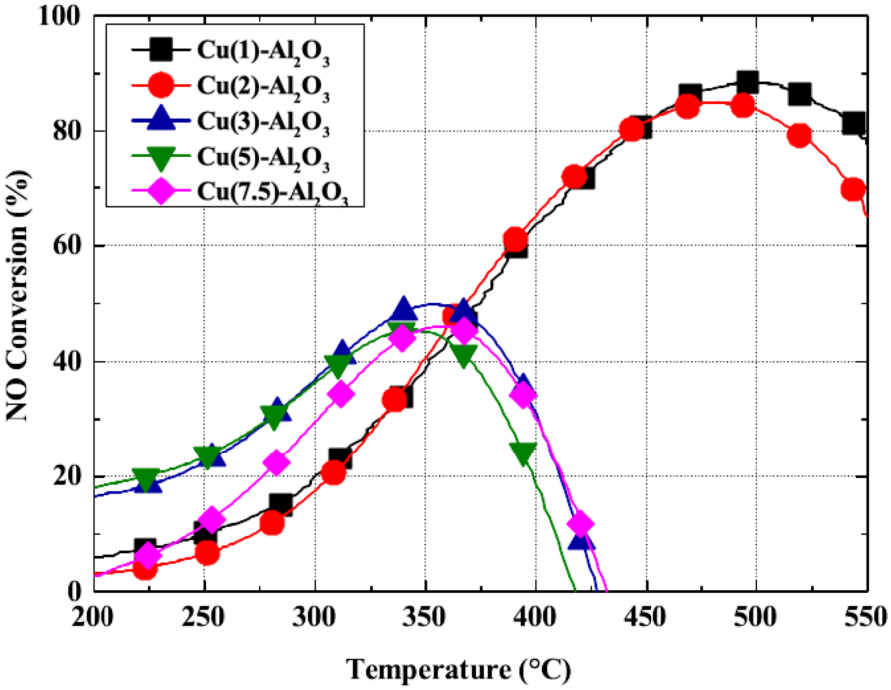

414

415 **Figure 9:** NO conversion profiles of the prepared Cu(x)-Al_2O_3 catalysts in the NH_3-SCR of NO.

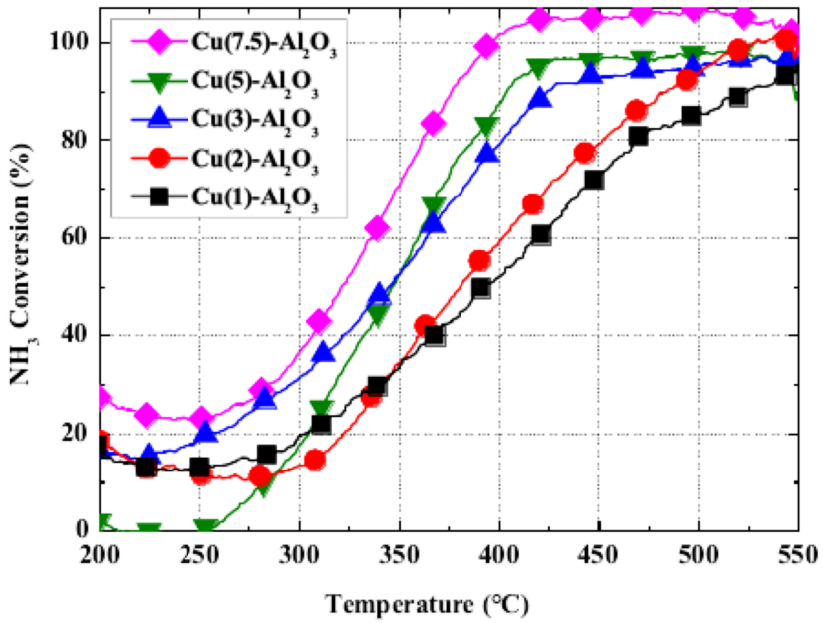

416

417 **Figure 10:** NH_3 conversion profiles of the prepared Cu(x)-Al_2O_3 catalysts in the NH_3-SCR of

418 NO.

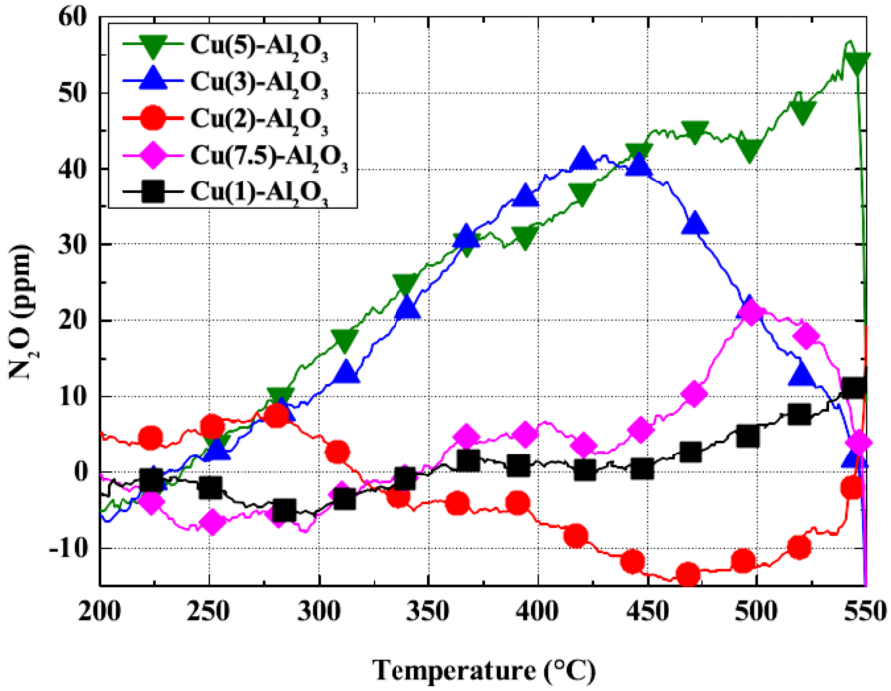

Figure 11: N_2O emission profiles during the NH_3-SCR of NO on Cu(x)-Al_2O_3 catalysts.

3.2.2 Selective catalytic Oxidation of NH_3

The oxidation profiles of NH_3 in the presence of 3.5% water vapor of the prepared catalysts Cu(x)-Al_2O_3 are presented in **figure 12**. The studied reaction is as follows (IV):

$$\mathbf{4NH_3 + 3O_2 \rightarrow 2N_2 + 6H_2O\ (IV)}$$

For all catalysts, it is noted that ammonia oxidation increases with the increase in temperature. For the Cu(3)-Al_2O_3, Cu (5)-Al_2O_3 and Cu(7.5)-Al_2O_3 catalysts, a gradual increase in NH_3 oxidation from 200 °C to 400 °C was recorded. But above 400 °C, the oxidation of NH_3 decreases slightly. On the other hand, for Cu(1)-Al_2O_3 and Cu(2)-Al_2O_3 a gradual slower increase of the NH_3 conversion was recorded from 250 ° C to 550 ° C. These two catalysts are much less active towards ammonia oxidation as we have already seen previously in NH_3-SCR of NO. The catalytic activity of the catalyst Cu(1)-Al_2O_3 and Cu(2)-Al_2O_3 in the oxidation of NH_3 could be related to the highly dispersed CuO on the support which are reduced at low temperature T = 130 °C. According to (Gang et al., 1999) complete oxidation of NH_3 was obtained at 350 °C on

445 Cu(10%)-γAl_2O_3 catalyst with N_2 selectivity of 90%. Liang et al., 2012 obtained similar results
446 for Cu(10%)-γAl_2O_3 catalysts prepared by different copper precursors (nitrate, acetate and
447 sulphate) and calcined at 500 °C and 600 °C. They showed that a mixture of CuO and $CuAl_2O_4$
448 species is formed on the various Cu(10%)-γAl_2O_3 catalysts. On the other hand, the dispersion and
449 the nature of the copper species have a significant influence on the activity of the catalysts.
450 Indeed, the highly dispersed CuO nanoparticles on the support are responsible for the high
451 activity of Cu(10%)-γAl_2O_3 catalysts. Lenihan and Curtin (2009) using lower levels of copper
452 (Cu(3.4%)/γ-Al_2O_3) found conversions of the order of 100% in NH_3.

453 The nature of the copper precursor and the method of preparation were found to be
454 determinants in the formation of active copper species in the NH_3-SCO. For example, a sulphate
455 precursor leads to the formation of $CuAl_2O_4$, whereas CuO of higher crystallinity is formed using
456 an acetate compared to a nitrate precursor (Jung et al., 2017). However, the nature of the active
457 species in NH_3- SCO has not been fully verified yet. Gang et al., 2000 claimed that the surface
458 $CuAl_2O_4$ spinel phase is responsible for the higher catalytic activity relative to CuO. A study
459 conducted by Liang et al., 2012 has shown that a mixture of CuO and $CuAl_2O_4$ phases is formed
460 on the various Cu (10%) - γAl_2O_3 catalysts. On the other hand, the dispersion and the nature of
461 the copper species have a significant influence on the activity of the catalysts. Indeed, CuO
462 nanoparticles highly dispersed on the support and easily reduced at low temperature are
463 responsible for the high conversion of NH_3.

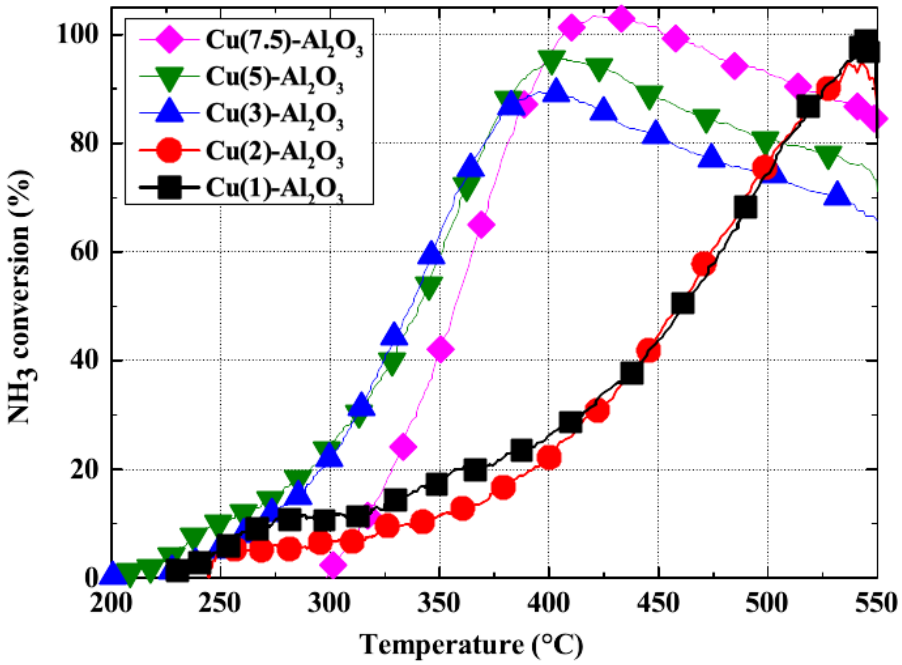

Figure 12: NH_3 oxidation profiles of Cu(x)-Al_2O_3 catalyst.

Figures 13, 14 and **figure 15** presents the selectivity profiles towards NO, N_2O and N_2 respectively obtained in the NH_3-SCO reaction. N_2 is the desired gas product, while NO and N_2O are undesired by-products. The Cu(1)-Al_2O_3 and Cu(2)-Al_2O_3 catalysts have N_2 selectivity close to 95% over the temperature range of 200-400 °C. Additionally, the transition metal oxides have been widely studied in the scientific literature (Jablonska and Palkovits, 2016; Sazonova et al., 1996). This type of catalysts showed higher selectivity to N_2, however, they need significantly higher operation temperatures as high as 300–500 °C than noble metal catalysts. For the three others Cu(x)-Al_2O_3, selectivities towards N_2 are much lower. At 550 °C (**Figure 16**), 48%, 40%, 30% of selectivity towards NO were measured for (Cu(7.5)-Al_2O_3, Cu(5)-Al_2O_3, Cu(3)-Al_2O_3) respectively.

The NH_3-SCO method is an effective method for oxidizing NH_3 into N_2. The overall selectivity into N_2 was close to 100% for Cu(1)-Al_2O_3 and above 95% for Cu(2)-Al_2O_3 over all the temperature while for the other three catalysts, N_2 selectivity remains as high as 95% only at

temperature below 350°C, as reported by (Jabłońska et al.,2017; 2018). Highly dispersed CuOx favor moderate activity but N_2 selectivity up to 550 °C in NH_3-SCO (Chmielarz et al., 2005). In a similar work (Dong et al. 2013) showed that nitrogen gas was primarily formed by the direct dissociation of the NO produced by the oxidation of the adsorbed NH_3 (Dong et al., 2014).

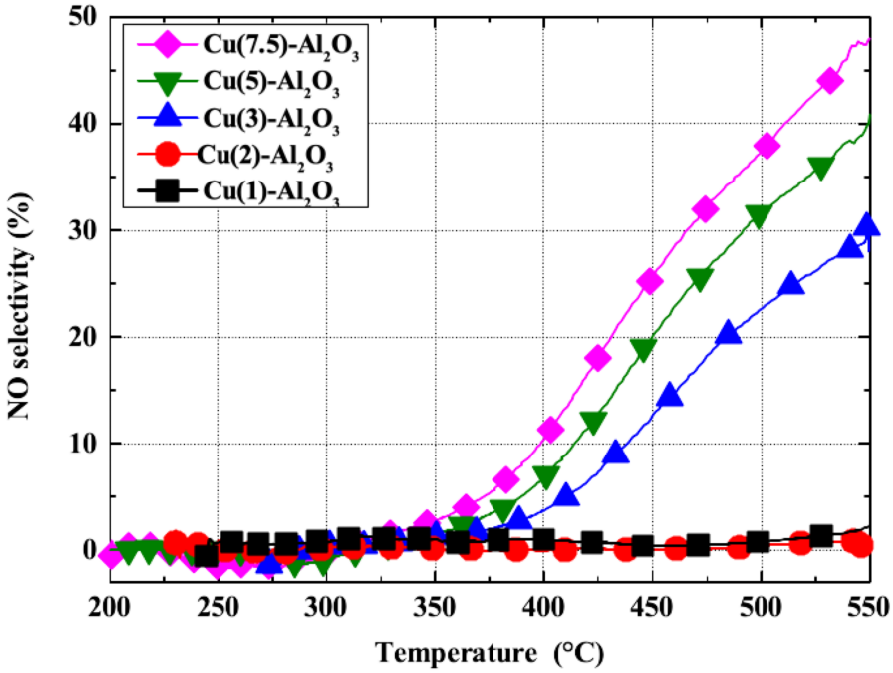

Figure 13: NO selectivity profiles obtained for NH_3-SCO performed over Cu(x)-Al_2O_3 catalysts.

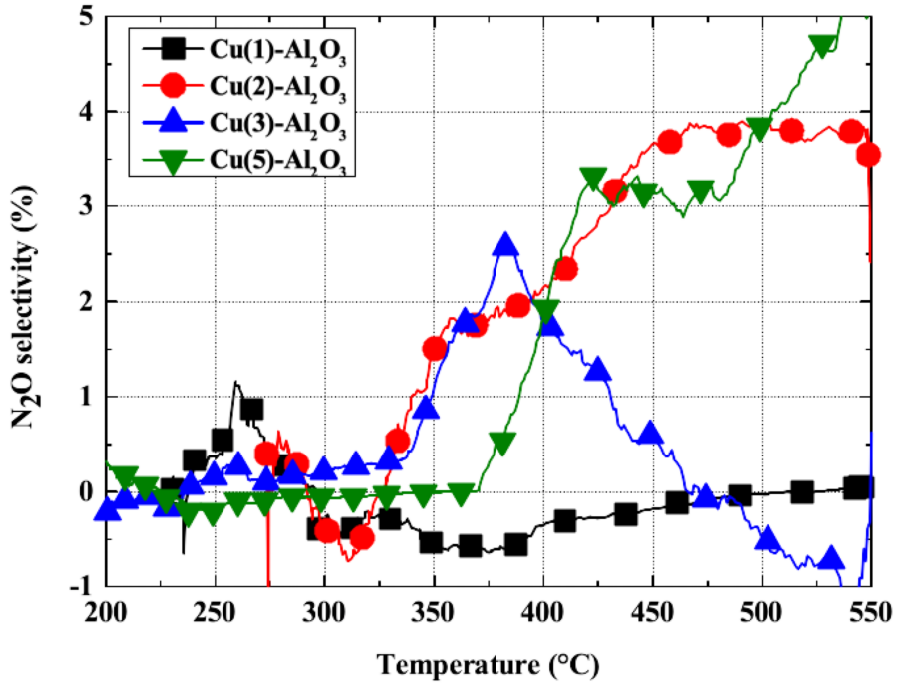

Figure 14: N_2O selectivity profiles obtained for NH_3-SCO performed over Cu(x)-Al_2O_3 catalysts.

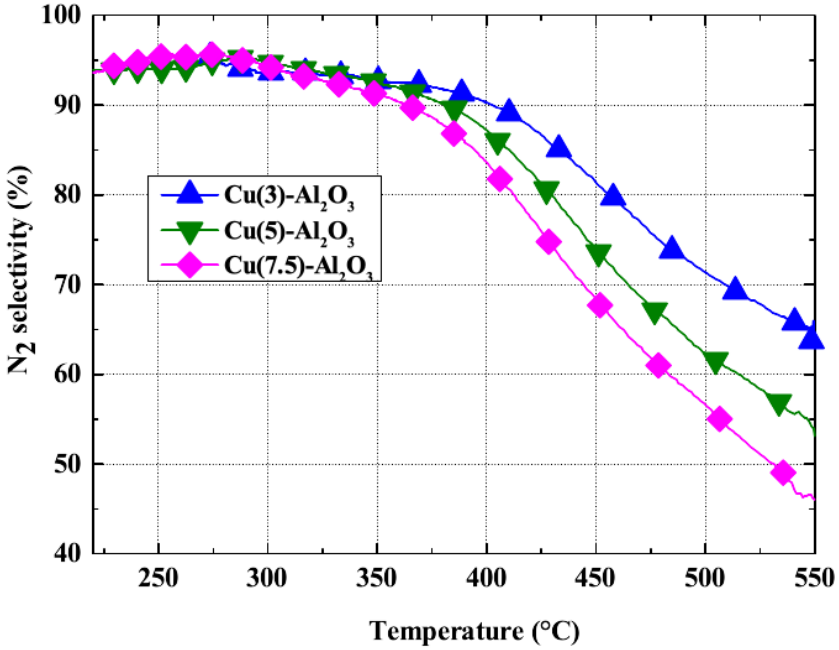

Figure 15: N_2 selectivity profiles obtained for NH_3-SCO performed over Cu(x)-Al_2O_3 catalysts.

4 Conclusion

Copper-supported η-Al_2O_3 catalysts have prepared and tested in the selective catalytic reduction of NO by NH_3 and in the selective catalytic oxidation of NH_3.The impregnation/evaporation method has successfully dispersed the copper species on the surface of the alumina for the low copper contents; Cu(1)-Al_2O_3 and Cu(2)-Al_2O_3 catalysts. The XRD showed that the introduction of an additional amount of copper leads to the destruction of the alumina structure when copper content exceeded 3% wt.%. The Cu(3)-Al_2O_3, Cu(5)-Al_2O_3 and Cu (7.5) -Al_2O_3 catalysts contain mainly large CuO particles. Cu(2)-Al_2O_3 and Cu(1)-Al_2O_3 catalysts have interesting NO conversion to N_2 in the NH_3-SCR of NO. This activity could be related essentially to the small CuO clusters deposited on the alumina surface and $CuAl_2O_4$ species. For NH_3-SCO, the catalyst Cu(1)-Al_2O_3 and Cu(2)-Al_2O_3 exhibit similar behavior resulting in the conversion of NH_3 to N_2 of about 100% at T > 500 ° C. This conversion could be attributed to CuO nanoparticles highly dispersed on the support and easily reduced at low temperature.

Ethics approval and consent to participate “Not applicable.

Consent for publication “Not applicable”.

Competing interests The authors declare that they have no known competing financial interests or personal relationships that could have appeared to influence the work reported in this paper.

Availability of data and materials “Not applicable”.

Funding “Not applicable”.

Authors' contributions

Nawel Jraba: analyzed the data and write the complete paper.

HassibTounsi, Thabet Makhlouf and Gerard Delahay: gave this idea of work.

All authors read and approved the final manuscript.

REFERENCES

Águila G, Gracia F, Araya P (2008) CuO and CeO_2 catalysts supported on Al_2O_3, ZrO_2, and SiO_2 in the oxidation of CO at low temperature. Appl Catal A 343(1-2) : 16-24. https://doi.org/10.1016/j.apcata.2008.03.015

Boroń P, Rutkowska M, Gil B, Marszałek B, Chmielarz L, Dzwigaj S (2019) Experimental Evidence of the Mechanism of Selective Catalytic Reduction of NO with NH_3 over Fe-Containing BEA Zeolites. Chem Sus Chem 12(3): 692-705. https://doi.org/10.1002/cssc.201801883.

Buvaneswari G, Aswathy V, Rajakumari R (2015) Comparison of color and optical absorbance properties of divalent ion substituted Cu and Zn aluminate spinel oxides synthesized by combustion method towards pigment application. Dyes Pigm 123 : 413-419. https://doi.org/10.1016/j.dyepig.2015.08.024.

Carre S, Tapin B, Gnep NS, Revel R and Magnoux P (2010) Model reactions as probe of the acid–base properties of aluminas: Nature and strength of active sites. Correlation with physicochemical characterization. Appl Catal A 372 (1) : 26-33. https://doi.org/10.1016/j.apcata.2009.10.005.

Chaudhary RG, Sonkusare VN, Bhusari GS, Mondal A, Shaik DP, Juneja HD (2018) Microwave-mediated synthesis of spinel $CuAl_2O_4$ nanocomposites for enhanced electrochemical and catalytic performance. Res Chem Intermediat 44(3) : 2039-2060. https://doi.org/10.1007/s11164-017-3213-z.

Chmielarz L, Kuśtrowski P, Rafalska-Łasocha A, Dziembaj R (2005) Selective oxidation of ammonia to nitrogen on transition metal containing mixed metal oxides. Appl Catal B Environ 58: 235–244. https://doi.org/10.1016/j.apcatb.2004.12.009.

Cychosz KA, Thommes M (2018) Progress in the physisorption characterization of nanoporous gas storage materials. Eng 4(4) : 559-566. https://doi.org/10.1016/j.eng.2018.06.001.

Damma D, Ettireddy PR, Reddy BM, Smirniotis PG (2019) A review of low temperature NH_3-SCR for removal of NOx. Catalysts 9(4) : 349. https://doi.org/10.3390/catal9040349.

Dong CD, Chen CW, Hung CM (2014). Catalytic performance and characterization of copper-based Rare earth composite materials for selective catalytic oxidation reaction with simulated synthetic ammonia stream. J Adv Oxid Technol 17(2) : 352-358. https://doi.org/10.1515/jaots-2014-0220.

Fierro G, Lojacono M, Inversi M, Porta P, Lavecchia R, Cioci F (1994) A study of anomalous temperature-programmed reduction profiles of Cu_2O, CuO, and CuO-ZnO catalysts. J Catal 148(2) : 709-721. https://doi.org/10.1006/jcat.1994.1257.

Forzatti P (2001) Present status and perspectives in de-NOx SCR Catalysis. Appl Catal A 222: 221-236. https://doi.org/10.1016/S0926-860X(01)00832-8.

Friedman RM, Freeman JJ, Lytle FW (1978) Characterization of $CuAl_2O_3$ catalysts. J Catal 55 (1): 10-28. https://doi.org/10.1016/0021-9517(78)90181-1.

Gang L, Anderson BG, Van Grondelle J, Van Santen RA (2000) NH_3 oxidation to nitrogen and water at low temperatures using supported transition metal catalysts. Catal Today 61(1-4) : 179-185. https://doi.org/10.1016/S0920-5861(00)00375-8.

Gang L, Van Grondelle J, Anderson BG, Van Santen RA (1999) Selective low temperature NH_3 oxidation to N_2 on copper-based catalysts. J Catal 186(1) : 100-109. https://doi.org/10.1006/jcat.1999.2524.

Gao F, Szanyi J (2018) On the hydrothermal stability of Cu/SSZ-13 SCR. Appl Catal A 560 185-194. https://doi.org/10.1016/j.apcata.2018.04.040.

Goldbach M, Roppertz A, Langenfeld P, Wackerhagen M, Füger S, Kureti S (2017) Urea decomposition in selective catalytic reduction on $V_2O_5/WO_3/TiO_2$ catalyst in diesel exhaust. Chem Eng Technol 40(11) : 2035-2043. https://doi.org/10.1002/ceat.201700261.

Hamoud HI, Valtchev V, Daturi M (2019) Selective catalytic reduction of NOx over Cu-and Fe-exchanged zeolites and their mechanical mixture. Appl Catal B 250 : 419-428. https://doi.org/10.1016/j.apcatb.2019.02.022.

Hansen TK, Høj M, Hansen BB, Janssens TV, Jensen AD (2017) The Effect of Pt Particle Size on the Oxidation of CO, $C3H_6$, and NO Over Pt/Al_2O_3 for Diesel Exhaust Aftertreatment. Top Catal 60 (17-18) : 1333-1344. https://doi.org/10.1007/s11244-017-0818-9.

Hoyong J, Jung H, Park J, and Jung KD. (2017) Surface Modification of η–Al_2O_3 by SiO_2 Impregnation to Enhance Methanol Dehydration Activity. Bull Korean Chem Soc 38(3) : 307-312. https://doi.org/10.1002/bkcs.11081.

Il'chenko, Ivanovna N (1976) Catalytic oxidation of ammonia. Russ Chem Rev 4512 1119. https://doi.10.1070/RC1976v045n12ABEH002765.

Jabłońska M (2020) Progress on Selective Catalytic Ammonia Oxidation (NH_3-SCO) over Cu–Containing Zeolite-Based Catalysts. Chem Cat Chem 12 (18) : 4490-4500. https://doi.org/10.1002/cctc.202000649.

Jabłońska M, Beale AM, Nocuń M, Palkovits R (2018) Ag-Cu based catalysts for the selective ammonia oxidation into nitrogen and water vapour. Appl Catal B 232: 275-287. https://doi.org/10.1016/j.apcatb.2018.03.029.

Jabłońska M, Wolkenar B, Beale AM, Pischinger S, Palkovits R (2018). Comparison of Cu-Mg-Al-Ox and Cu/Al_2O_3 in selective catalytic oxidation of ammonia (NH_3-SCO). Catal Commun 110 : 5-9. https://doi.org/10.1016/j.catcom.2018.03.003.

Jabłońska M, Nocuń M, Gołąbek K, Palkovits R (2017) Effect of preparation procedures on catalytic activity and selectivity of copper-based mixed oxides in selective catalytic oxidation of ammonia into nitrogen and water vapour. Appl Surf Sci 423: 498-508. https://doi.org/10.1016/j.apsusc.2017.06.144.

591 Jabłońska M, Palkovits R (2016) Copper based catalysts for the selective ammonia oxidation
592 into nitrogen and water vapour-recent trends and open challenges. Appl Catal B 18 : 332-351.
593 https://doi.org/10.1016/j.apcatb.2015.07.017.
594 Jabłońska M (2015) Selective catalytic oxidation of ammonia into nitrogen and water vapour
595 over transition metals modified Al_2O_3, TiO_2 and ZrO_2. Chem Pap 69 : 1141-1155.
596 https://doi.org/10.1515/chempap-2015-0120.
597 Jeong SM, Jung SH, Yoo KS, Kim SD (1999) Selective catalytic reduction of NO by NH_3 over a
598 bulk sulfated CuO/γ-Al_2O_3 catalyst. Ind Eng Chem Res 38 (6) : 2210-2215.
599 https://doi.org/10.1021/ie9807147.
600 Jo H, Jung H, Park J and Jung K D (2017) Surface Modification of η–Al_2O_3 by SiO_2
601 Impregnation to Enhance Methanol Dehydration Activity. Bull Korean Chem Soc 38 (3): 307-
602 312. https://doi.org/10.1002/bkcs.11081
603 Jones JM, Pourkashanian M, Williams A, Backreedy RI, Darvell LI, Simell P, Heiskanen K and
604 Kilpinen P (2005) The selective oxidation of ammonia over alumina supported catalysts–
605 experiments and modelling. Appl Catal B 60 (1-2): 139-146.
606 https://doi.org/10.1016/j.apcatb.2004.11.013
607 Jraba N, Tounsi H, Makhlouf T (2018) Valorization of aluminum chips into γ-Al_2O_3 and η-Al_2O_3
608 with high surface areas via the precipitation route. Waste Biomass Valori 9 (6): 1003-1014.
609 https://doi.org/10.1007/s12649-016-9786-8.
610 Jung Y, Shin YJ, Pyo YD, Cho CP, Jang J, Kim G (2017) NOx and N_2O emissions over a Urea-
611 SCR system containing both V_2O_5-WO_3/TiO_2 and Cu-zeolite catalysts in a diesel engine. Chem
612 Eng J 326 : 853-862. https://doi.org/10.1016/j.cej.2017.06.020.
613 Kong T, Jia Y, Zhang L, Shu H, Chang X, Kuang W, Luo M (2020) CuO–MoO_2–CeO_2 yolk–
614 albumen–shell catalyst supported on γ-Al_2O_3 for denitration with resistance to SO_2. J Mater Sci
615 55 (9): 3833-3844. https://doi.org/10.1007/s10853-019-04216-x.

Kröcher O (2018) Selective catalytic reduction of NOx. Catalysts 8 : 459. https://doi.org/10.3390/catal8100459.

Kwak JH, Tonkyn R, Tran D, Mei D, Cho SJ, Kovarik L, ... and Szanyi J (2012) Size-dependent catalytic performance of CuO on γ-Al_2O_3 : NO reduction versus NH_3 oxidation. ACS Catal 2 (7): 1432-1440. https://doi.org/10.1021/cs3002463.

Lai JK, Wachs IE (2018) A perspective on the selective catalytic reduction (SCR) of NO with NH_3 by supported V_2O_5–WO_3/TiO_2 catalysts. ACS Catal 8 (7) : 6537-6551. https://doi.org/10.1021/acscatal.8b01357.

Lambert CK (2019) Perspective on SCR NO x control for diesel vehicles. React Chem Eng 4 (6) : 969-974. https://doi.org/10.1016/j.apcata.2018.04.040.

Le TA, Kim TW, Lee SH and Park ED (2017) CO and CO_2 methanation over Ni catalysts supported on alumina with different crystalline phases. Korean J. Chem. Eng 34(12): 3085-3091. https://doi.org/10.1007/s11814-017-0257-0

Lenihan S, Curtin T (2009) The selective oxidation of ammonia using copper-based catalysts: The effects of water. Catal Today 145(1-2) : 85-89. https://doi.org/10.1016/j.cattod.2008.06.017.

Liang C, Li X, Qu Z, Tade M, Liu S (2012) The role of copper species on Cu/γ-Al_2O_3 catalysts for NH_3–SCO reaction. Appl Surf Sci 258 (8) : 3738-3743. https://doi.org/10.1016/j.apsusc.2011.12.017.

Mayer RW, Melzer M., Hävecker M, Knop-Gericke A, Urban J, Freund HJ, Schlögl R, (2003) Comparison of oxidized polycrystalline copper foil with small deposited copper clusters in their behavior in ammonia oxidation: an investigation by means of in situ NEXAFS spectroscopy in the soft X-ray range. Catal lett 86 (4): 245-260. https://doi.org/10.1023/A:1022624303979

Nikoofar K, Shahedi Y and Chenarboo FJ (2019) Nano alumina catalytic applications in organic transformations. Mini Rev Org Chem 16 (2): 102-110. https://doi.org/10.2174/1570193X15666180529122805.

Nova I, Tronconi E (Eds.) (2014) Urea-SCR technology for deNOx after treatment of diesel exhausts. N Y Springer 5. https://doi.org/10.1007/978-1-4899-8071-7.

Osman AI and Abu-Dahrieh JK (2018) Kinetic investigation of η-Al_2O_3 catalyst for dimethyl ether production. Catal Lett 148 (4): 1236-1245. https://doi.org/10.1007/s10562-018-2319-2

Osman AI, Abu-Dahrieh JK, Abdelkader A, Hassan NM, Laffir F, McLaren M and Rooney D (2017) Silver-modified η-Al_2O_3 catalyst for DME production. J Phy Chem C 121 (45): 25018-25032. https://doi.org/10.1021/acs.jpcc.7b04697.

Panahi PN, Delahay G (2017) Activity of γ–Al_2O_3-based Mn, Cu, and Co oxide nanocatalysts for selective catalytic reduction of nitric oxide with ammonia. Turk J Chem 41(2) : 272-281. https://doi.org/10.3906/kim-1605-50.

Peintinger MF, Kratz M J andBredow T (2014) Quantum-chemical study of stable, meta-stable and high-pressure alumina polymorphs and aluminum hydroxides. J Mater Chem A 2 : 13143-13158. https://doi: 10.1039/C4TA02663B.

Petitto C, Mutin HP, Delahay G (2013) Hydrothermal activation of silver supported alumina catalysts prepared by sol–gel method: Application to the selective catalytic reduction (SCR) of NOx by n-decane. Appl Catal B 134: 258-264. https://doi.org/10.1016/j.apcatb.2013.01.018.

Piumetti M, Bensaid S, Fino D and Russo N (2015) Catalysis in Diesel engine NOx aftertreatment: a review. Catal Struct React 1(4): 155-173. https://doi.org/10.1080/2055074X.2015.1105615.

Sazonova NN, Simakov AV, Nikoro TA, Barannik GB, Lyakhova VF, Zheivot VI ... and Veringa H (1996) Selective catalytic oxidation of ammonia to nitrogen. React Kinet Catal Lett 57(1) : 71-79. https://doi.org/10.1007/BF02076122.

Shibata, G., Eijima, W., Koiwai, R., Shimizu, K. I., Nakasaka, Y., Kobashi, Y., Kubota, Y., Ogura, M., and Kusaka, J. (2019). NH_3-SCR by monolithic Cu-ZSM-5 and Cu-AFX catalysts:

665 Kinetic modeling and engine bench tests. Catalysis Today, 332: 59-63.
666 https://doi.org/10.1016/j.cattod.2018.06.023
667 Ström L, Carlsson PA, Skoglundh M, Härelind H (2018) Surface species and metal oxidation
668 state during H_2-assisted NH_3-SCR of NOX over alumina-supported silver and
669 indium. Catalysts 8(1): 38. https://doi.org/10.3390/catal8010038.
670 Sun M, Liu J, Song C, Ogata Y, Rao H, Zhao X, Xu H, and Chen Y (2019) Different Reaction
671 Mechanisms of Ammonia Oxidation Reaction on Pt/Al_2O_3 and $Pt/CeZrO_2$ with Various Pt
672 States. ACS Appl Mater Interfaces 11(26) : 23102-23111.
673 https://doi.org/10.1021/acsami.9b02128.
674 Svintsitskiy DA, Kibis LS, Stadnichenko AI, Slavinskaya EM, Romanenko AV, Fedorova EA ...
675 and Boronin AI (2020) Insight into the nature of active species of Pt/Al_2O_3 catalysts for low
676 temperature NH_3 oxidation. Chem Cat Chem 12 (3) : 867-880.
677 https://doi.org/10.1002/cctc.201901719.
678 Usberti N, Jablonska M, Di Blasi M, Forzatti P, Lietti L, Beretta A (2015) Design of a high-
679 efficiency NH_3-SCR reactor for stationary applications. A kinetic study of NH_3 oxidation and
680 NH_3-SCR over V-based catalysts. Appl Catal B 179 : 185-195.
681 https://doi.org/10.1016/j.apcatb.2015.05.017.
682 Villamaina R, Nova I, Tronconi E, Maunula T, Keenan M (2019) Effect of the NH_4NO_3 Addition
683 on the Low-T NH_3-SCR Performances of Individual and Combined Fe-and Cu-Zeolite
684 Catalysts. Emiss Control Sci Technol 5(4) : 290-296. https://doi.org/10.1007/s40825-019-00140-
685 3.
686 Walker A (2016) Future challenges and incoming solutions in emission control for heavy duty
687 diesel vehicles. Top Catal 59 (8-9) : 695-707. https://doi.org/10.1007/s11244-016-0540-z.
688 Xie G, Liu Z, Zhu Z, Liu Q, Ge J, Huang Z (2004) Simultaneous removal of SO_2 and NOx from
689 flue gas using a CuO/Al_2O_3 catalyst sorbent: II. Promotion of SCR activity by SO_2 at high
690 temperatures. J Catal 224(1) : 42-49. https://doi.org/10.1016/j.jcat.2004.02.016.

Xin Y, Li Q, Zhang Z (2018) Zeolitic materials for DeNOx selective catalytic reduction. Chem Cat Chem 10(1): 29-41. https://doi.org/10.1002/cctc.201700854.

Yan JY, Lei GD, Sachtler WMH, Kung HH (1996) Deactivation of Cu/ZSM-5 catalysts for lean NOx reduction: characterization of changes of Cu state and zeolite support. J Catal 161(1) : 43-54. https://doi.org/10.1006/jcat.1996.0160.

Yuan X, Liu H, Gao Y (2015) Diesel engine SCR control: current development and future challenges. Emiss Control Sci Technol 1(2) : 121-133. https://doi.org/10.1007/s40825-015-0013-z.